Available online at www.sciencedirect.com
SCIENCE DIRECT®
Journal of Nuclear Materials 329–333 (2004) 1017–1021
journal of nuclear materials
www.elsevier.com/locate/jnucmat

Control of phosphorus inter-granular segregation in ferritic steels

Z. Lu [a,*], R.G. Faulkner [a], N. Sakaguchi [b], H. Kinoshita [b], H. Takahashi [b], P.E.J. Flewitt [c]

[a] Institute of Polymer Technology and Materials Engineering, Loughborough University, Loughborough, Leicestershire LE11 3TU, UK
[b] Center for Advanced Research of Energy Technology, Hokkaido University, North 13, West 8, Sapporo 060-8628, Japan
[c] Berkeley Centre, Magnox Electric, Berkeley, Gloucestershire GL13 9PB, UK

Abstract

Low- and high-alloy ferritic steels, 2.25Cr1Mo and E911, were irradiated by 250 keV Ni^+ ions at 300 °C to study radiation-induced inter-granular phosphorus segregation behaviour and the effect of hafnium on radiation-induced segregation. Irradiations were carried out in an ion accelerator to a dose of 0.452 dpa for 2.25Cr1Mo and 0.305 dpa for E911 and E911+1%Hf. Grain boundary phosphorus segregation was detected by using field emission gun transmission electron microscopy with an energy dispersive X-ray analyzer. The phosphorus segregation at boundaries after irradiation in the high-alloy steel is higher than that in the low-alloy steel. Hafnium can suppress radiation-induced segregation to approximately one-sixth of the level in hafnium-free materials. A model to predict radiation-induced segregation in foil-samples is presented. Site competition between carbon and phosphorus is taken into consideration. The predicted results show good agreement with experimental data.

1. Introduction

Ferritic steels can be used to manufacture the nuclear reactor pressure vessel (RPV) in fission reactors and are also important candidates for structural materials in fusion reactors. The RPV is one of key structural components for the safety of nuclear power plants, because it houses the nuclear fuel. During service, a great number of neutrons are produced and bombard the internal surfaces of the reactor pressure vessel. The interaction of incident energetic particles and lattice atoms results in concentration gradients of point defects between matrix and sinks, e.g. grain boundaries and free surface. This causes solute element re-distribution near sinks. The segregation of P to grain boundaries is thought to reduce grain boundary cohesion, causing the material to fail through inter-granular embrittlement [1]. Radiation-induced phosphorus segregation behaviour was reviewed in [2]. The solute drag model [3,4] and rate theory [5] have been applied successfully to predict radiation-induced segregation (RIS). In other work, it was interesting to note that some oversized elements can suppress chromium depletion and nickel enrichment at grain boundaries in austenitic steel [6–8]. However, no study on the prevention of radiation-induced segregation in ferritic steel has yet been reported.

In this study, radiation-induced phosphorus inter-granular segregation behaviour and the effect of element Hafnium (Hf) on radiation-induced phosphorus segregation in low- and high-alloy ferritic steels is investigated. A solute drag model for predicting radiation-induced inter-granular segregation in foil samples is described. The predicted results are compared with experimental data.

* Corresponding author. Tel.: +44-1509 263171x4048; fax: +44-1509 223949.
E-mail address: zheng.lu@lboro.ac.uk (Z. Lu).

0022-3115/$ - see front matter © 2004 Elsevier B.V. All rights reserved.
doi:10.1016/j.jnucmat.2004.04.127

2. Experimental

Low- and high-alloy ferritic steels, 2.25Cr1Mo(Fe–2.28Cr–0.086C–0.46Mn–0.3Si–0.077P–0.0009S–0.15Ni–1.00Mo–0.011Sn–0.005As–0.021Sb, wt%) and E911 (Fe–9.16Cr–0.105C–1.00W–0.072N–0.35Mn–0.2Si–0.007P–0.003S–0.23Ni–0.68Nb–1.01Mo–0.23V, wt%), were used in this study. 2.25Cr1Mo steel, doped with 0.077 wt% P, was manufactured by induction melting under argon atmosphere. The ingots were hot-rolled to 10 mm diameter rods and they were then austenitised at 1150 °C for 2 h, furnace-cooled to an intermediate temperature of 950 °C, held there for 30 min and then air-cooled to room temperature. Finally they were austenitised at 1050 °C for 2 h and air-cooled. E911 was supplied by Corus as normalised at 1060 °C for 1 h then air-cooled.

TEM discs (3 mm) were prepared from the two steels. Electro-polishing was applied to produce thin areas. Hafnium (Hf, 1 at.%) was implanted in E911 at room temperature. The ion current was kept to about 1 μA and the accelerating voltage was 250 kV. E911 with and without Hf (marked by E911+Hf and E911, respectively) and 2.25Cr1Mo were irradiated by heavy ions (Ni^+) in the ion beam line attached to the multi-beam high voltage electron microscopy (ARM 1300), Hokkaido University, Japan. Irradiations were carried out under the dose rate of 2.36×10^{-5} dpa/s at 300 °C. Doses for E911 and 2.25Cr1Mo were 0.305 and 0.452 dpa, respectively. Ni concentrations in both steels increase to about 4 wt% due to high dose Ni^+-radiation.

After irradiation, thinning of TEM foils was carried out by an ion-milling instrument in order to remove surface amorphous-layers induced by ion implantation. Grain boundary composition was measured using a field-emission-gun analytical TEM (JEOL 2010F) equipped with an energy dispersive X-ray analyzer (Noran Inc. VOYAGER system). The nominal spot size is 0.5 nm.

3. Modeling of radiation-induced inter-granular segregation in foil samples

A solute drag model was developed to predict radiation-induced inter-granular segregation in bulk dilute solute alloys [3], which shows a good agreement with radiation-induced phosphorus segregation in different materials under different radiation conditions [4]. In this study, radiation was carried out with TEM foil samples. The difference between radiation in foil and bulk sample should be taken into consideration. Here we assumed a grain in bulk samples (see Fig. 1(a)). During radiation, freely migrating point defects migrate toward GB from the matrix. If we consider only a very narrow region in the grain, as shown in Fig. 1(a), nearly all defects will migrate toward the GB. If this narrow regime is cut out from bulk samples, i.e. a foil sample, as shown in Fig. 1(b), there are two additional free surfaces, compared to the case in bulk samples. During radiation of foil samples, the defects will migrate not only to GBs but also to the free surfaces. The areas of the free surfaces are greater than those of the GBs. Therefore, some of the solute elements may migrate to free surfaces in foil sample.

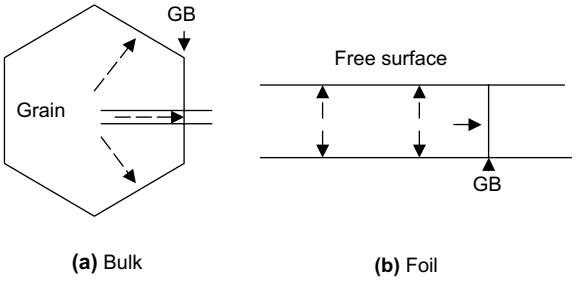

Fig. 1. Schematic illustration of radiation-induced freely migrating defect flux to grain boundaries in bulk samples (a) and in foil samples (b).

Radiation-induced solute segregation in foil samples can be written:

$$C_{\mathrm{br}}^{\mathrm{S}j}=C_{\mathrm{g}}^{\mathrm{S}j}\frac{E_{\mathrm{b(S}j)}^{\mathrm{ip}}}{E_{\mathrm{f}}^{\mathrm{p}}}\left[\frac{C_{\mathrm{g}}^{\mathrm{S}j}\exp\left(\frac{E_{\mathrm{b(S}j)}^{\mathrm{ip}}}{kT}\right)}{\sum_j C_{\mathrm{g}}^{\mathrm{S}j}}\exp\left(\frac{E_{\mathrm{b(S}j)}^{\mathrm{ip}}}{kT}\right)\right]\times\left[1+\frac{L(t_{\mathrm{f}})\mathrm{BGF}(\eta)}{A_{\mathrm{p}}D_{\mathrm{p}}k_{\mathrm{dp}}^2}\exp\left(\frac{E_{\mathrm{f}}^{\mathrm{p}}}{kT}\right)\right]\quad(j=1,2),$$

where $C_{\mathrm{br}}^{\mathrm{S}j}$ is the maximum concentration of solute j on the grain boundary, $C_{\mathrm{g}}^{\mathrm{S}j}$ is the grain concentration, $E_{\mathrm{b(S}j)}^{\mathrm{ip}}$ is the self-interstitial-impurity binding energy, $E_{\mathrm{f}}^{\mathrm{p}}$ is the point-defect formation energy, B is the proportion of freely migrating defects in the bulk matrix, G is the point defect generation rate, $F(\eta)$ is the recombination rate, A_{p} is a constant associated with the vibrational entropy of atoms around point-defects, D_{p} is the diffusion coefficient of point-defects in the matrix, k_{dp}^2 is the sink strengthen for point-defects, $L(t_{\mathrm{f}})$ is the proportion of freely migrating defects in foil samples, which is function of foil thickness.

$$L(t_{\mathrm{f}})=\frac{t_{\mathrm{f}}C_{\mathrm{g}}^{\mathrm{S}j}\exp\left(\frac{E^{\mathrm{GB}}}{kT}\right)}{t_{\mathrm{f}}C_{\mathrm{g}}^{\mathrm{S}j}\exp\left(\frac{E^{\mathrm{GB}}}{kT}\right)+SC_{\mathrm{g}}^{\mathrm{S}j}\exp\left(\frac{E^{\mathrm{S}}}{kT}\right)},$$

where t_{f} is foil thickness, S is the linear size of the free surface (S equal to grain size for TEM foils), E^{S} is surface energy, E^{GB} is grain boundary energy: this value is obtained from random boundary tilted about $\langle1\,1\,0\rangle$ in α-Fe [9], T is radiation temperature.

The kinetics of radiation-induced segregation can be expressed by

$$\frac{C_{\mathrm{br}}^{\mathrm{S}j}(t)-C_{\mathrm{g}}^{\mathrm{S}j}}{C_{\mathrm{br}}^{\mathrm{S}j}-C_{\mathrm{g}}^{\mathrm{S}j}}=1-\exp\left(\frac{4D_{\mathrm{c}}^{\mathrm{ip}}t}{\alpha_{\mathrm{n}}^{2}d^{2}}\right)\operatorname{erfc}\left(\frac{2\sqrt{D_{\mathrm{c}}^{\mathrm{ip}}t}}{\alpha_{\mathrm{n}}d}\right),$$

where $C_{\mathrm{br}}^{\mathrm{S}j}(t)$ is the solute concentration at radiation time t, $D_{\mathrm{c}}^{\mathrm{ip}}$ is the diffusion coefficient of the complexes, α_{n} is the maximum enrichment ratio, given by $\alpha_{\mathrm{n}}=C_{\mathrm{br}}^{\mathrm{S}j}/C_{\mathrm{g}}^{\mathrm{S}j}$ and d is the thickness of the grain boundary.

Site competition is also considered in this model. It is assumed that the solutes i and j first segregate to the grain boundary independently by solute-self-interstitial complex mechanism to obtain segregation levels $C_{\mathrm{br}}^{\mathrm{S}i}$ and $C_{\mathrm{br}}^{\mathrm{S}j}$, then re-distribute there in proportion to their binding energies with the grain boundary, The effect is expressed by

$$C_{\mathrm{br}}^{\mathrm{S}j}(t)^{*}=C_{\mathrm{br}}^{\mathrm{S}j}(t)\left[\frac{C_{\mathrm{g}}^{\mathrm{S}j}\exp\left(\frac{Q_{\mathrm{S}j}}{kT}\right)}{C_{\mathrm{g}}^{\mathrm{S}i}\exp\left(\frac{Q_{\mathrm{S}i}}{kT}\right)+C_{\mathrm{g}}^{\mathrm{S}j}\exp\left(\frac{Q_{\mathrm{S}j}}{kT}\right)}\right],$$

where $C_{\mathrm{br}}^{\mathrm{S}j}(t)^{*}$ is the final level of irradiation-induced grain boundary segregation for solute j, $Q_{\mathrm{S}i}$ and $Q_{\mathrm{S}j}$ are the binding energies of the grain boundary with solutes i and j, respectively, and $C_{\mathrm{g}}^{\mathrm{S}i}$ and $C_{\mathrm{g}}^{\mathrm{S}j}$ are matrix concentration of solutes i and j, respectively.

In addition, microstructural factors such as grain size and dislocation density are accommodated in this model [3].

4. Results and discussion

Both E911 and 2.25Cr1Mo steels have a lath martensite microstructure. Transmission electron microscopy revealed that there are a few Nb-rich carbides in E911 (from tens to hundreds of nm) and no apparent precipitation in 2.25Cr1Mo prior to the irradiation at 300 °C, see Figs. 2 and 3, respectively.

In E911 steel, the bulk concentration of P is very low (ca. 0.007 wt%). Prior to radiation, the phosphorus concentration at prior austenite grain boundaries measured by FEGTEM equipped with EDS X-ray analyzer is about 0.17 wt%. After the radiation at 300 °C, the P concentration at GBs is up to 1.66 wt% (see Fig. 4). This shows that ion-radiation induces strong phosphorus segregation to the GB. Three to four grain boundaries were checked from each sample.

A similar radiation-induced P segregation behaviour is also observed in 2.25Cr1Mo steel. The P bulk concentration in the steel is 10 times higher than that in E911 steel, up to 0.077 wt%. Prior to radiation, the P concentration at the GB is 0.27 wt%, a little higher than in E911 steel. After the radiation at 300 °C, the P intergranular concentration increases to 0.91 wt%, far lower than in E911 steel (see Fig. 5).

The phenomenon can be explained by site competition. It is well known that there is site competition between free carbon and phosphorus in steels during their segregation to GB [10,11]. The carbon composition in both steels is similar (a little higher in E911 than in 2.25Cr1Mo). However, the formation of carbides in E911 during manufacture or heat treatment decreases

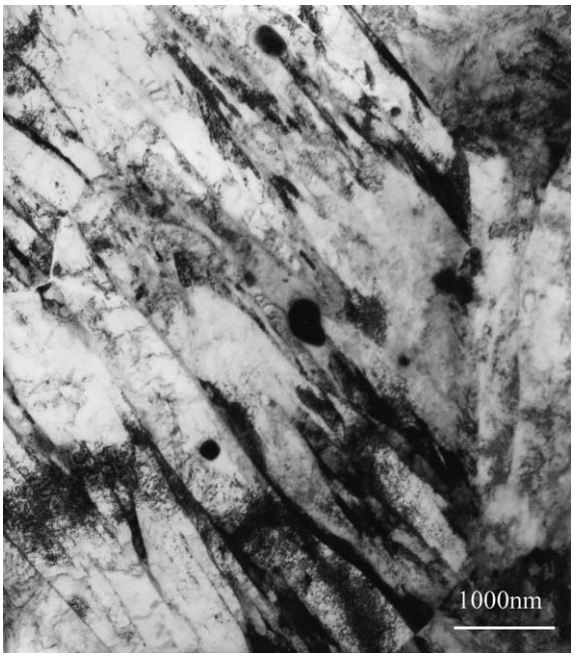

Fig. 2. The microstructure of unirradiated E911 steel.

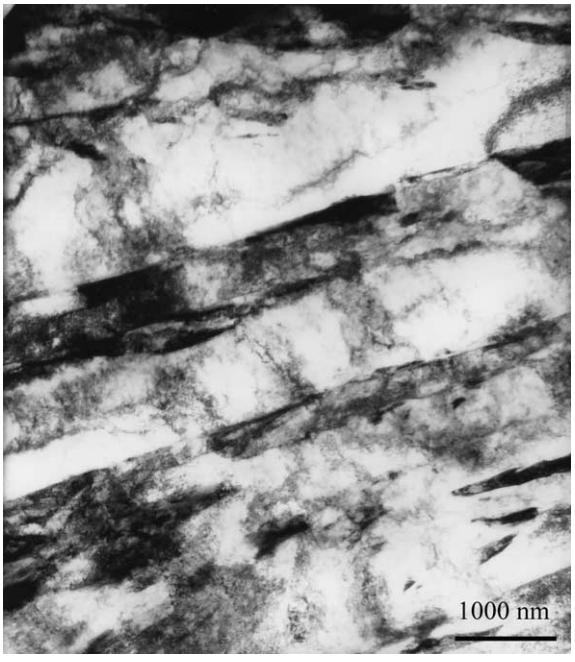

Fig. 3. The microstructure of unirradiated 2.25Cr1Mo steel.

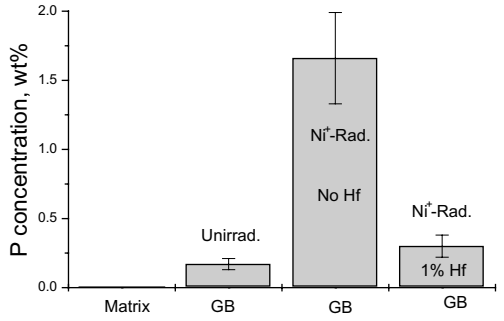

Fig. 4. Phosphorus concentration in unirradiated and radiated E911 steel.

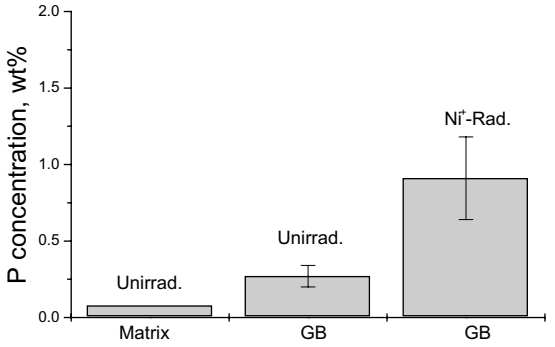

Fig. 5. Phosphorus concentration in unirradiated and radiated 2.25Cr1Mo steel.

the free carbon concentration in matrix. But no carbides are observed in 2.25Cr1Mo steel, so the free carbon concentration in 2.25Cr1Mo is higher than in E911. Thus it is easy to understand why the P segregation in low P E911 is higher than in high P 2.25Cr1Mo.

The effect of Hf on RIS was studied by comparing the RIS in E911 and E911+Hf which were irradiated in the same conditions, e.g. temperature, dose and dose rate. The P grain boundary segregation in E911+Hf is reduced to 0.3 wt%, only about one-fifth compared to E911, as shown in Fig. 4. This means that Hf can suppress effectively radiation-induced P segregation.

Most of the point defects produced by a primary knock-on may mutually recombine, annihilate at sinks such as surfaces, grain boundaries, dislocations, or form vacancy platelets and interstitial clusters. Those vacancies and interstitials surviving energetic displacement events and becoming free to migrate over large distances relative to cascade dimensions are called freely migrating point-defects, and are only a small proportion of those defects generated by the cascades. These are of great importance in radiation-induced segregation. P is an undersized atom in ferritic steel and may migrate to the GB through P-interstitial complexes. For oversized impurities, the binding energy of impurity–vacancy complexes increases with increasing impurity atom radius [12]. The atomic radius of Hf is greater than any other elements in the steels. So Hf can trap easily vacancies, resulting in reduced mobility of vacancies and enhancement of vacancy–interstitial recombination in the matrix. In situ TEM observations of void and interstitial loop growth give support to this assumption [6,8]. Thus, Hf can suppress phosphorus segregation toward GB by decreasing the population of self-interstitials and vacancies.

The solute drag model described in Section 3 is applied to predict the RIS in 2.25Cr1Mo, E911 and E911+Hf. The P enrichment ratios are calculated by ratioing the experimentally measured or theoretically predicted concentration on the boundary with the bulk concentration in weight percent. It should be pointed out that the actual P grain boundary concentration should be much higher than those determined by FEGTEM microanalysis because of its limited spatial resolution. An analytical convolution method established by Faulkner et al. [13] to quantify the true solute grain boundary segregation is used here. The corrected boundary concentrations of P in E911 and 2.25Cr1Mo are 0.28 wt% (unirradiated sample, the measured value is 0.17 wt%), 2.68 wt% (radiated, no Hf, 1.66 wt%), 0.49 wt% (radiated, 1% Hf, 0.3 wt%) and 0.44 wt% (unirradiated, 0.27 wt%), 1.46 wt% (radiated, 0.91 wt%), respectively. The corresponding enrichment ratios are shown in Fig. 6. Most of the parameters used in this modeling can be found in [4]. The grain size and dislocation density are 10 μm and 6.4×10^{14} m^{-2}, respectively. The thickness of foils used in this study is about 80 nm, so $L(t_f)$ is 0.01. For irradiated 2.25Cr1Mo and E911, when free carbon concentrations are 100 and 1 appm, the predicted results are reasonably consistent with experimental values. Experimentally determined radiation-induced proportion of freely migrating defects B is

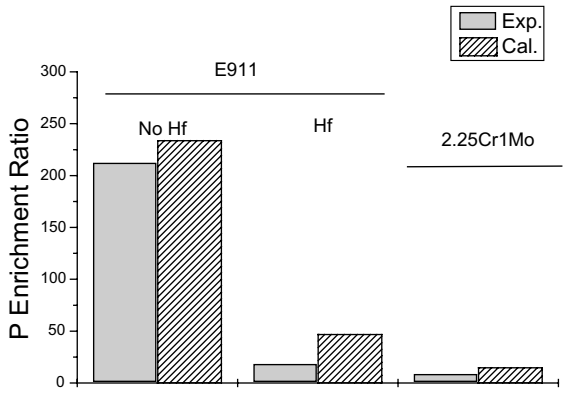

Fig. 6. Comparison between experimental P segregation ratios and predicted results.

about 1% [14]. Molecular dynamics simulations [15] show the higher B value, about 15%. In this study, B in 2.2.Cr1Mo and E911 is thought to be 0.01. When the B in E911+Hf decreases to 1% of the value in 2.25Cr1Mo and E911, the predicted results show a good agreement with experimental data, seen in Fig. 6. These comparisons verify the effectiveness of the model.

5. Summary

Ni^{+}-irradiations induce P inter-granular segregation in both E911 and 2.25Cr1Mo steels. The segregation of P in E911 is much higher than in 2.25Cr1Mo owing to site competition between C and P. The addition of Hf can suppress the segregation P to the GB. A solute drag model is presented in this study to predict radiation-induced segregation in Hf-implanted and Hf-free foil specimens and the predicted results show good agreement with experimental data.

Acknowledgements

This study is sponsored by EPSRC (contracts GR/R37999 and GR/R01682) and JSPS, Japan.

References

[1] S.G. Druce, G. Gage, G. Jordan, Acta Metall. 34 (1986) 641.
[2] C.A. English, S.R. Ortner, G. Gage, W.L. Server, S.T. Rosinski, ASTM-STP 1405 (2001) 151.
[3] R.G. Faulkner, S. Song, P.E.J. Flewitt, M. Victoria, P. Marmy, J. Nucl. Mater. 255 (1998) 189.
[4] R.G. Faulkner, P.E.J. Flewitt, Z. Lu, ASTM-STP 1447, submitted for publication.
[5] S.G. Druce, C.A. English, A.J.E. Foreman, R.J. McElroy, I.A. Vatter, C.J. Bolton, J.T. Buswell, R.B. Jones, ASTM-STP 1270 (1996) 119.
[6] T. Kato, H. Takahashi, M. Izumiya, Mater. Trans. JIM 32 (1991) 921.
[7] T. Kato, H. Takahashi, M. Izumiya, J. Nucl. Mater. 189 (1992) 167.
[8] T. Kato, H. Takahashi, M. Izumiya, J. At. Energy Soc. Jpn. 34 (1992) 889.
[9] D. Wolf, Philos. Mag. A 62 (1990) 447.
[10] M. Guttman, P. Dumoulin, M. Wayman, Metall. Trans. A 13A (1982) 1693.
[11] H. Hansel, H.J. Grabke, Scr. Metall. 20 (1986) 1641.
[12] R.G. Faulkner, S.H. Song, P.E.J. Flewitt, Mater. Sci. Technol. 12 (1996) 904.
[13] R.G. Faulkner, T.S. Morgan, E.A. Little, X-Ray Spectrom. 23 (1994) 195.
[14] V. Naundorf, M.-P. Macht, H. Wollenberger, J. Nucl. Mater. 186 (1992) 227.
[15] R.G. Faulkner, D.J. Bacon, S. Song, P.E.J. Flewitt, J. Nucl. Mater. 271&272 (1999) 1.